Surface Science 155 (1985) 327–340
North-Holland, Amsterdam

THEORETICAL STUDIES OF FAST He ATOM SCATTERING FROM A W{100} SURFACE

Che-Chen CHANG and Barbara J. GARRISON *

Department of Chemistry, The Pennsylvania State University, University Park, Pennsylvania 16802, USA

and

Henning B. NIELSEN and T.A. DELCHAR

Physics Department, University of Warwick, Coventry CV4 7AL, Warwickshire, UK

Received 11 September 1984; accepted for publication 31 December 1984

Theoretical calculations of the scattering of fast neutral He atoms from W{100} are presented which are directly compared to the results from recent experiments of Nielsen and Delchar. The experiments which were performed for He atom energies between 150 and 1000 eV, and for incident polar angles between 0° and 65° as measured from the surface normal, displayed peaks in the polar angle distributions at 72°, 56° and ±10°. The results from classical dynamics calculations are employed here to explain the scattering phenomena that give rise to these peaks in the polar distributions. The calculations indicate that the peak at 72° is primarily due to scattering from the first layer W atoms. The peaks at ±10° and 56° are unusual in that there are a multitude of different collision paths that result in the He atom being scattered into the same final angle. The peaks at ±10° result from He atoms scattering mainly from the second, third and fourth layers of W atoms. The He atoms are focused on the outward path into the near normal direction by two first and two second layer W atoms. Subsurface scattering is also responsible for the peak at 56°. In this case the channel of first and second layer W atoms that focuses the outgoing He atoms is oriented at 54.7° with respect to the surface normal. It is proposed that slight variations of the experimental data from the calculated values are due to surface reconstruction of W{100} and that a more thorough analysis could reveal the microscopic nature of this structure.

1. Introduction

The scattering of ions in the energy range of 500–5000 eV has been used as a probe of the geometrical arrangement of atoms on surfaces [1]. Historically noble gas ions (He^+ or Ne^+) rather than neutral atoms have been used as the probing particles since they are easier to produce, collimate and detect. This leads to complications in interpreting the scattered intensities since many of

* Camille and Henry Dreyfus Teacher–Scholar.

0039-6028/85/$03.30 © Elsevier Science Publishers B.V.
(North-Holland Physics Publishing Division)

the ions are neutralized at the surface and are consequently generally not detected. Much of the information that could be gained about surface structure is lost. Different approaches have been employed to overcome this problem. Buck uses a time-of-flight mass spectrometer so that both the scattered ions and neutral atoms are detected [2]. Several investigators are using alkali ions (e.g. Li^+ or K^+) as the probe since the neutralization probability is small and most of the scattered particles are detected [3–5]. Another approach used by Nielsen and Delchar is to scatter noble gas neutral atoms from a surface and to detect the neutral atoms [6]. Here the ionization probability is negligible and virtually all the scattered particles are detected.

These latter experiments on fast He atom scattering from W{100} have yielded polar angle distributions which exhibit peaks that cannot be readily attributed to specific scattering mechanisms [6]. For He scattering in-plane along the ⟨110⟩ azimuth of W{100}, peaks in the polar distributions are observed at angles of 72°, 56°, 10° and −10°. All angles are given with respect to the surface normal and a negative polar angle indicates that the particles are scattered back toward the incident beam. The peak at ~72° corresponds to the minimum total scattering angle (i.e. the angle between the incident and scattered beams) which has been observed in other experiments and in theoretical calculations. The ±10° peaks shift position slightly with beam energy and dominate the polar angle distribution for near normal angles of incidence. The peak at 56° is most apparent for near normal incident scattering.

Due to the complexity of the atom scattering process, these data are best interpreted with the aid of theoretical calculations which model the scattering event using classical dynamics [7,8]. This theoretical approach is particularly suited to modeling this set of experimental data since a neutral He beam was used as the probe, and the neutral scattered flux was detected by a channeltron. Thus, reneutralization of the scattered particle does not need to be considered when making quantitative comparisons between the measured and calculated results. In addition, several experimental angular distributions were generated for each angle of incidence. This fact means that more of the calculated scattered particles may be compared to the experimental data than if the particles were collected at only one final angle.

In this paper He scattering from W{100} has been modeled theoretically as a function of the energy and angle of incidence of the primary beam. The results indicate that there should be four major peaks in the polar angle distributions between −20° and 90° corresponding to those observed experimentally by Nielsen and Delchar [6]. A detailed analysis of the atomic trajectories indicates that the peak near 72° arises mainly from scattering from the first layer of W atoms. The peaks at ±10° result from He atoms which are scattered mainly from W atoms in the second, third, and fourth layers. Upon exiting the surface the scattered He atoms are channeled by two first and two second layer atoms into the upward direction. Of note, is that for near normal

angles of incidence the fourth layer scattering is comparable in magnitude to that from the second and third layers. In addition, there is no *one* dominant collision path of scattering from each layer. A He atom is able to penetrate the surface through one of the holes, rattle around through the crystal and then exit through another hole in the near normal direction. Finally, the peak at 56° is due to subsurface scattering where the exiting He atom is channeled by first and second layer atoms. This channel is oriented at 54.7° from the surface normal. A reciprocity argument was used by Nielsen and Delchar [6] to dismiss this channel as giving rise to the peak at 56°.

2. Description of the calculation

A classical dynamics procedure was employed to simulate He atom scattering from W{100}. The W surface was generated using a bcc microcrystallite of tungsten atoms with the {100} crystal face exposed. The primary particle was allowed to impinge at a specific incident polar angle along the ⟨110⟩ azimuth. In our model, Hamilton's equations of motion are numerically integrated to determine the positions and momenta of all the particles as a function of time. In previous simulations of both secondary ion mass spectrometry and ion scattering spectrometry (ISS) experiments, we have assumed that all the particles simultaneously interact via a sum of pairwise additive potentials [7–9]. In a separate study we have found that identical results for ISS simulations can be obtained by neglecting the interactions among the surface atoms [10,11]. Therefore, the only interactions assumed in the calculations presented here are between the incident particle and the substrate atoms. The primary particle, however, is allowed to interact simultaneously with all the substrate atoms within a radius of ~ 3.8 Å. At this distance the potential is $\sim 10^{-3}$ eV. A Molière potential using a Thomas–Fermi screening radius [12] is used to describe the interaction between the He atom and each W atom. As discussed below there may be some basis for adjusting the value of the screening parameter.

The He atoms bombard along the ⟨110⟩ azimuth with energies between 150 and 1000 eV and at polar angles of 0° to 65° from the surface normal in order to reproduce the experimental conditions. The He atoms must be uniformly aimed at all points on the surface. From symmetry arguments it can be shown that the triangle depicted in fig. 1 is an irreducible zone which fully represents the infinite unreconstructed {100} surface for bombardment along the ⟨110⟩ azimuth. Many of the He trajectories traverse a long lateral distance inside the W{100} crystal. To describe accurately these He atom motions a large microcrystallite is required to avoid edge effects. After considerable testing, it was found that a crystal four atomic layers thick and with the surface area shown in fig. 1 was adequate to contain all of the significant scattering events.

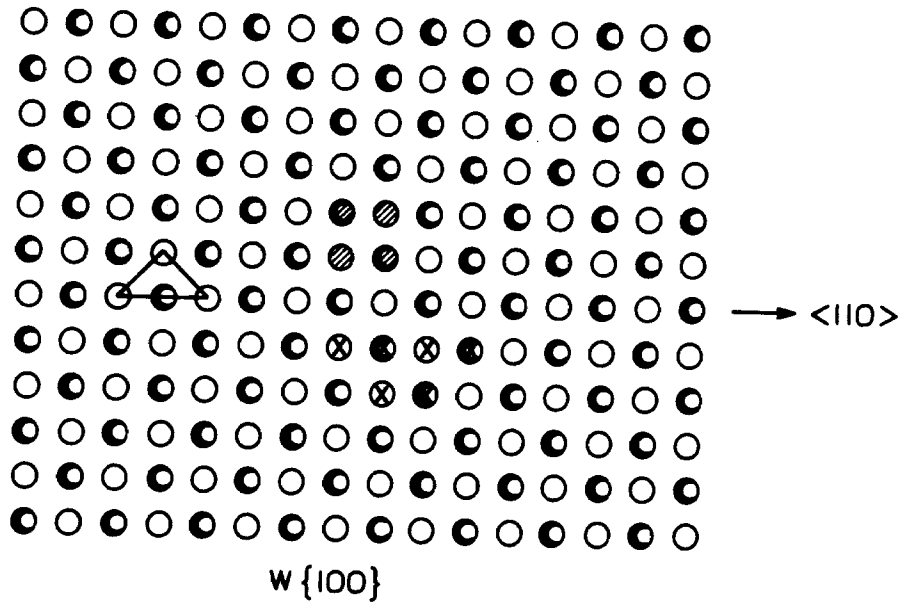

Fig. 1. The unreconstructed W{100} crystal face. The shaded circles represent atoms in the first layer and the open circles those in the second layer. The lattice constant is 3.16 Å. The atom sizes correspond to the distance of closest approach for a 250 eV He atom. The triangular region is the impact zone for incidence along the ⟨110⟩ azimuth. The four hashed atoms are typical of those that can channel He atoms nearly straight up from the surface. The six atoms marked with a cross form the channel for the particles to exit at 56°. In both cases the highlighted atoms are representative of and are not the specific atoms that channel the He atoms.

For each set of initial conditions $(\sim 2\text{–}15)\times 10^4$ trajectories are calculated with the incident He atom aimed randomly within the triangular surface region of fig. 1. For each collision sequence that results in reflection from the surface the initial conditions, final energy and angles, collision time and maximum depth of penetration in the solid are stored for subsequent analysis. The polar angle distributions are plotted with a resolution of $\pm 7°$ in the polar direction. This value is slightly larger than the experimental value, but allows more reliable statistics to be obtained with fewer collision trajectories.

The main uncertainty in this calculation is the surface structure of W{100} during the experiments. Although W{100} is known to reconstruct, the reconstruction geometries are not precisely known [13]. Nielsen and Delchar believe that they have chosen experimental conditions such that the surface has a bulk terminated geometry [6]. As a starting point an unreconstructed W{100} surface is used in the calculations. As discussed below, the major features of the experimental spectra are well-reproduced in the calculated results by this choice of geometry. The major discrepancy between the calculated and experi-

mental results is in the scattered intensity in the direction normal to the surface. Since the particles scattered in this direction are strongly influenced by the relative placements of the first and second layer atoms, either lateral or vertical displacements of the tungsten atoms could affect this scattering process.

3. Comparison of calculated and experimental results

The calculated and experimental polar angle distributions for He scattering at an energy of 250 eV and various angles of incidence are shown in fig. 2. In all the figures the polar angle in the abscissa refers to the exit angle of the He atoms and is measured with respect to the surface normal. Since the beam energy is invariant, the experimental primary beam flux and the collector efficiency are nearly constant for this set of experimental data. Therefore, direct intensity comparisons between the experimental and calculated results can be made. The $\theta_i = 65°$ curves have been peak normalized in fig. 2. The remainder of the intensities are then reported relative to this intensity. Several striking comparisons can be made between experiment and calculation. The agreement is quite good both with respect to the shape of the curves and the scaling between different curves. (The agreement in shape for the $\theta_i = 45°$ and 55° data improves significantly if these curves are also peak normalized.) A peak at the minimum total scattering angle (i.e. ~ 70°) and a pair of peaks at $\pm$ 10–20° are predicted. For $\theta_i = 35°$ the peaks at 70° and 10° are about equal in intensity; whereas, for $\theta_i = 65°$ the peak at 70° dominates. The calculated peak at 70° is approximately 5° closer to the surface normal than the experimental one. A slightly rougher surface (obtained either by increasing the distance between W atoms or by decreasing the effective size of the interaction potential) would move the position of this peak to a larger polar angle [14]. Calculations for a He energy of 250 eV at $\theta_i = 45°$ were performed using a Molière potential with a screening radius of 0.8 of the Thomas–Fermi value in order to determine the effect of the potential on the peak positions. There was only a negligible difference between this polar distribution and that shown in fig. 2. Inclusion of thermal effects into the calculation also did not significantly alter the polar distributions. The major discrepancy between the calculated and experimental distributions is in the region within ~ 20° of the normal direction. The calculated peak positions are slightly shifted outward and the calculated intensity at 0° is consistently lower than the experimental values. This difference could again be due to the choice of potential parameters or more likely could be an indication that there is surface reconstruction. As discussed below, the intensity from −10° to 10° has a large contribution from He atoms scattered from the third and fourth layers that are eventually channeled in the vertical direction. Changes in the arrangement of atoms in the first two layers should alter this scattered intensity.

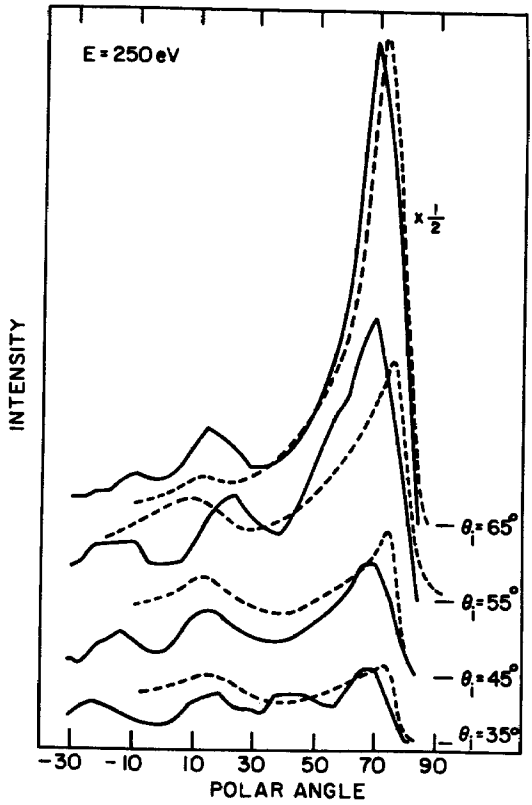

Fig. 2. Polar angle distributions of scattered He for various He atom angles of incidence θ_i. All angles refer to the exit angle of the He atom and are measured from the surface normal. In all cases the initial He energy is 250 eV and only particles scattered in-plane are collected. The solid lines are the calculated results. All curves have the same intensity scale with only the baselines displaced. The dashed lines are the experimental results from ref. [6], fig. 4. The experimental curve for $\theta_i = 65°$ is peak normalized to the calculated one. The remaining experimental intensities are determined from fig. 5 of ref. [6].

The comparisons between the calculated and experimental results for near normal angles of incidence are shown in fig. 3. Nielsen and Delchar could not detect scattered particles near the beam source because of experimental constraints; therefore, the peak at 10° is not observable for $\theta_i = 0°$ and 10°. Since the peak at 10° dominates the calculated polar angle distributions, it is difficult to make direct intensity comparisons. The same qualitative behaviour observed in the experimental distributions is seen in the calculated ones. The calculated distributions exhibit a broad peak at $\sim 56°$ for $\theta_i = 0°$. The intensity of this peak decreases as θ_i increases with the peak at $\sim 70°$ more noticeable as θ_i increases.

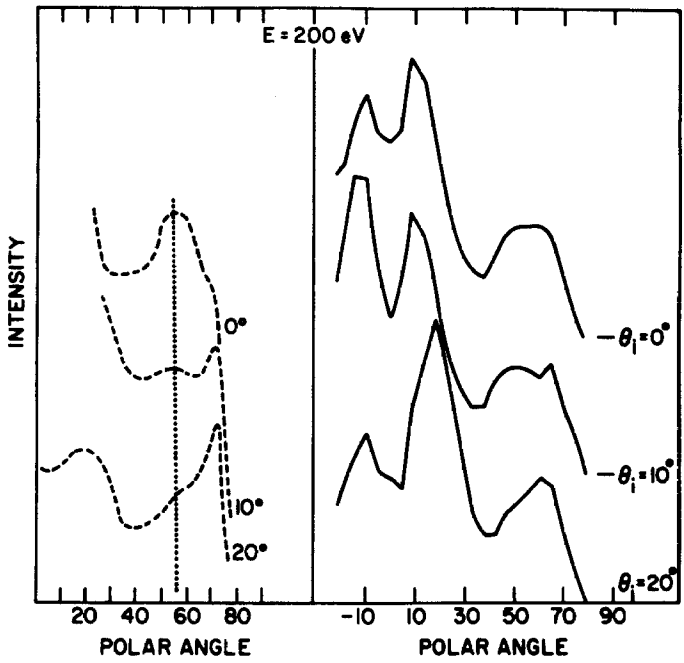

Fig. 3. Polar angle distributions of scattered He for various He atom angles of incidence θ_i. In all cases the initial He energy is 200 eV. The solid lines are the calculated results. All curves have the same intensity scale with only the baselines displaced. The dashed lines are the experimental results from ref. [6], fig. 3. In contrast to fig. 2, here there are no direct intensity comparisons (see text).

As a first step toward understanding the scattering mechanisms that give rise to each peak, the contribution to the scattered intensity from He atom collisions with each of the tungsten layers as a function of the incident angle θ_i is plotted in fig. 4. For $\theta_i \geqslant 35°$ the primary energy is 250 eV and for $\theta_i \leqslant 20°$ the primary energy is 200 eV so there is a slight discontinuity in the curves. The contribution to the scattered intensity into final polar angles between $-20°$ and 90° as a function of the incident polar angle is displayed in fig. 4a. We have neglected the scattered intensity between $-90°$ and $-20°$ since this polar angle regime was not examined in the experiments. The total reflection cross section is relatively high for $\theta_i \leqslant 20°$ because the He atom can not only easily penetrate the surface and scatter off atoms in deeper layers but also easily escape along one of the vertical channels. For $\theta_i \geqslant 35°$ there are fewer channels into which the He atoms can penetrate the surface. The contribution to the total reflection cross section from subsurface scattering for these larger incident angles is thus reduced. However, as θ_i increases from 35° and 65° the first layer scattering cross section increases. By examining particles which

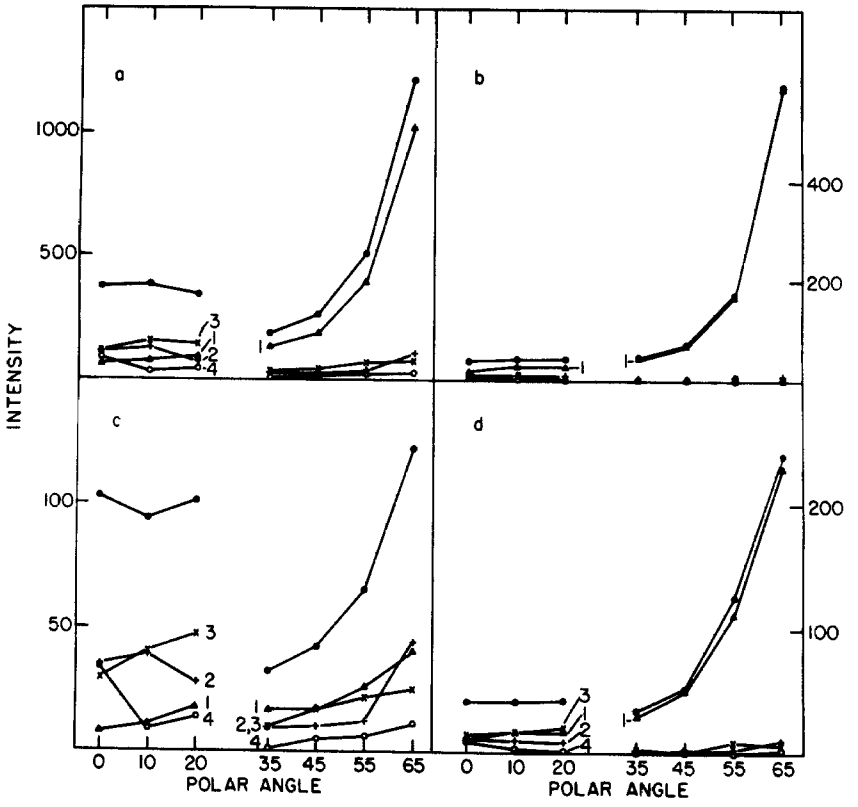

Fig. 4. Layer contributions to the scattering intensity as a function of angle of incidence, θ_i, of the He beam. For $\theta_i = 0°$, 10°, and 20° the He atom energy is 200 eV and for $\theta_i \geq 35°$ the energy is 250 eV. In some cases the curves in the figure are labeled with the layer number: (●) contribution from all four layers; (△) contribution from layer 1; (+) contribution from layer 2; (×) contribution from layer 3; (○) contribution from layer 4. (a) All final angles between −20° and 90°. (b) Final angles between 65° and 75°. (c) Final angles between 10° and 20°. (d) Final angles between 51° and 61°.

scatter into a narrow range of final polar angles the scattering mechanisms can be explored in more detail. For He atom reflection into a final angle between 65° and 75°, first layer scattering dominates as shown in fig. 4b. The peak at 70° corresponds to the minimum total scattering angle and has been observed and calculated by numerous investigators [14]. There is a large variation in the scattered intensity at 70° as a function of the incident angle. The intensity of scattered particles from the first layer is small at $\theta_i = 0°$ since the surface is quite open (see fig. 1) and many of the He atoms easily penetrate into the solid. Furthermore these atoms that end up in the solid are blocked from exiting at a polar angle of 70°. As the angle of incidence increases there are

fewer open spaces for the He atoms to penetrate and the scattering cross section increases due to more scattering from the first layer.

The peak at 10–20° is unusual in that subsurface scattering dominates the observed intensity as displayed in fig. 4c. Especially for near normal angles of incidence the scattering from the second and third layer atoms contributes 60–80% to the total intensity. In addition, the contribution from the fourth layer scattering is not negligible. Calculations performed at normal incidence on a microcrystallite with seven layers of W atoms showed that there is also a small contribution from fifth and sixth layer scattering. The reason for the large intensity at 10° is that there is a channel formed by two first layer atoms and two second layer atoms (a representative set of these atoms is marked in fig. 1) which focus the exiting atoms in an upward direction. By reciprocity it is also easier for an atom at normal incidence to penetrate into the solid than one oriented at a more oblique angle. Thus for normal incidence there is focusing on both the inward and outward paths of the He atom in the solid and the total cross section for the scattering into a final angle of 10–20° is large. In contrast to many previous simulations of ion (or neutral) scattering where it has been observed that one peak in the spectrum usually implies that only one scattering mechanism is operative [7,15,16], here there are numerous trajectories that result in a He atom which has a final polar angle of 10–20°. A sampling of these trajectories is shown schematically in fig. 5. The path can be as simple as one in which the atom penetrates straight in and back out the same channel, to one of a number of complex trajectories where the He atom is trapped between two layers before either moving deeper into or out of the crystal. For larger polar angles of incidence the mechanisms are similar to those for normal incidence although the number of oscillations between layers increases as the angle of incidence and the parallel component of momentum increases. Due to the crystal symmetry, for $\theta_i = 0°$ four peaks are observed with a polar angle of 10° and separated by 90° in the azimuthal direction. As the angle of incidence increases the relative intensity in the forward peak ($+10°$) increases and the intensity in the backward peak ($-10°$) decreases. This trend can be seen in figs. 2 and 3.

The peak at a final polar angle of 56° is by far the most difficult to explain since there is a large background which contributes to the intensity. The peak at 56° is barely present for $\theta_i \geq 35°$, an angle regime in which scattering from the first layer of W atoms dominates the polar distributions. Therefore, we looked for subsurface scattering mechanisms that would give rise to the peak at 56°. As in the case of the peak at $\pm 10°$ there are apparently many different mechanisms that allow the He atom to exit with a polar angle of $\sim 56°$. The common feature of each He atom path is that the back-scattered He atom collides with 3–4 tungsten atoms in the top two layers with a relative geometry similar to those marked by a cross in fig. 1. If one examines a three-dimensional model of the W{100} surface, these atoms define a channel at an angle

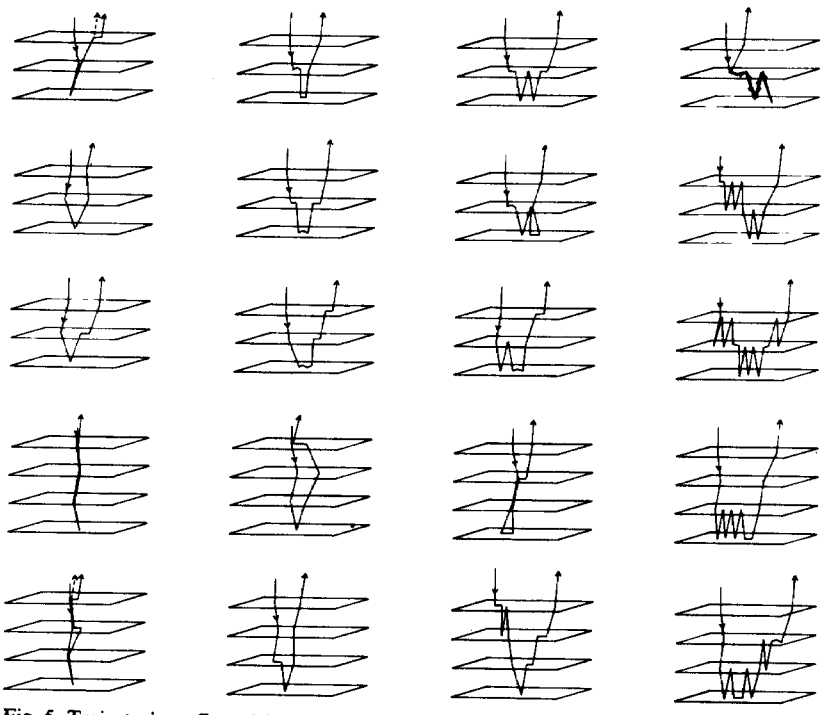

Fig. 5. Trajectories reflected from third and fourth layers that result in the He atom exiting with a final angle between 11° and 25°. The angle of incidence is 0° and the energy is 200 eV. These diagrams present a sampling of all the observed trajectories.

of 54.7° from the surface normal. Since focusing is dominated by first and second layer atoms there are a number of paths that the He atom may follow that originate with different initial steps but that terminate with a similar set of final channeling collisions. Due to the symmetry of the system, for $\theta_i = 0°$ there must also be a peak at $-56°$.

One set of experiments performed by Nielsen and Delchar on W{100} was for He atom scattering at $\theta_i = 50°$ as a function of He energy. The calculated and experimental polar distributions for this case are shown in fig. 6. The experimental data for each incident energy has been peak normalized to the calculated curve. In the calculated results the scattered intensity decreases with increasing energy. The experimental results exhibit the opposite behavior as the 350 and 1000 eV peak intensities are approximately 2–3 times larger than those for 150 and 250 eV. Since excellent agreement of intensities is obtained for constant energy studies as shown in fig. 2 and since other calculations [17] show that the cross section for reflection should decrease with increasing energy, we believe that our calculated results exhibit the correct dependence of

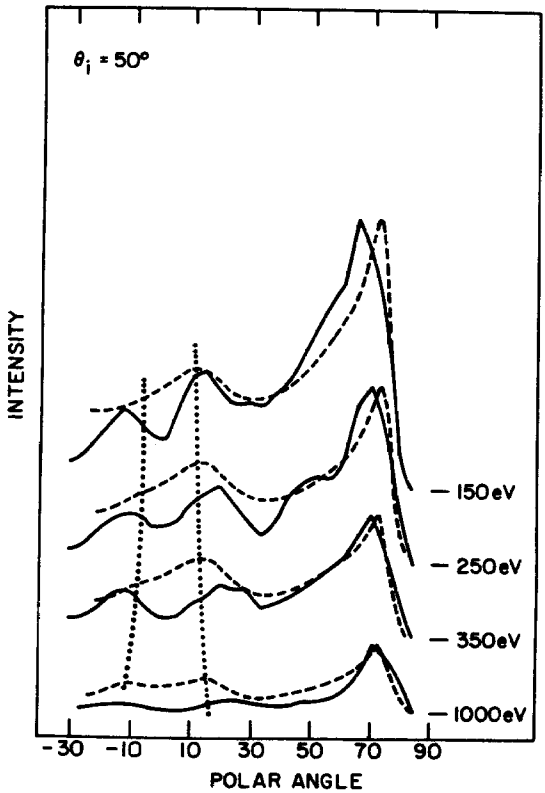

Fig. 6. Polar angle distributions as a function of He atom energy for $\theta_i = 50°$. The solid lines are the calculated results. All curves have the same intensity scale with only the baselines displaced. The dotted lines are the experimental results of fig. 2. ref. [6]. The curves have been peak normalized for each energy. The curves are plotted in the reverse order as in ref. [6]. The vertical lines mark the shift in the experimental peak position.

intensity on He energy. The measured experimental intensity includes not only the influence of the scattering cross section but also the dependence of the initial beam flux and the collection efficiency of the channeltron on energy. The channeltron efficiency is known to increase (probably non-linearly) with increasing particle energy in this energy range. This enhancement of the measured intensity by the channeltron for the larger He energies could account for the reversed intensity trend as a function of energy observed in the experimental data compared with that seen in the calculated results.

The channeltron efficiency could also affect the relative intensities within one polar distribution. The different scattering mechanisms result in slightly different final energies. For an initial energy of 200 eV and $\theta_i = 50°$, the He atoms scattered at 65° have ~ 190 eV of energy while those reflected normal

to the surface have energies between 150 and 190 eV. This difference is not large but the collection efficiency is unknown. Inclusion of an efficiency that increases with the energy in our calculations would result in the calculated intensities near 0° decreasing. This would tend to increase the discrepancy between the experimental and simulated results.

The overall shapes and relationship between the peak heights at 70° and 10° of the calculated polar distributions as a function of He energy are in excellent agreement with the experimental ones as seen in fig. 6. The major discrepancy is again for angles near 0° where the calculated values are smaller than the experimental ones. In agreement with the experimental results the calculated peak at ~ 10° shifts to larger polar angles as the He energy increases. At larger energies the effective sizes of the W atoms are reduced. Thus, they do not focus the exiting He atoms as effectively as they would for lower energy He atoms and, consequently, there is a larger spread in final angles.

4. Conclusions

Nielsen and Delchar have measured the polar angle distributions of neutral He atoms scattered from W{100} along the ⟨110⟩ direction as a function of He energy and polar angle of incidence. They observe peaks in the polar angle distributions that cannot be readily explained by simple geometrical scattering arguments. Classical dynamics simulations of the He atom scattering are performed in order to understand the structure in the measured polar angle distributions. The calculated polar distributions for a He energy of 250 eV and angles of incidence between 35° and 65° are in excellent agreement with the experimental curves. Quantitative comparisons of peak intensities can be made in this case since the experiments are carried out at constant energy and, thus, the experimental He atom detection efficiency is nearly constant. Peaks are observed in the polar distributions between −20° and 90° at angles of ~ 70° and ±10°, all measured with respect to the surface normal. The peak at ~ 70° is at the minimum total scattering angle for this system and arises primarily from He atom scattering from the first layer of W atoms. The peaks at ±10° are unusual in that there are a multitude of different trajectories that result in a He atom which exits the surface in the near normal direction. The He atom penetrates the solid to the second, third or fourth tungsten layer before reflecting and finally scattering out of the solid. The common feature in all the different mechanisms is that the He atom exits through a channel formed by two first and two second layer W atoms.

The polar angle distributions for near normal angles of incidence of the He atom exhibit intense peaks at ±10° as well as a peak at ~ 56°. A multitude of different trajectories also result in the He atom being scattered at 56°. In this case a channel formed by first and second layer atoms at an angle of 54.7°

from the surface normal provides the focusing mechanism for the scattered He atoms as they leave the solid. Finally, the polar angle distributions for a constant angle of incidence of 50° are calculated as a function of He energy from 150 to 1000 eV. The calculated distributions agree well in overall shape with the experimental curves. Quantitative comparisons cannot be made because the detection efficiency of the channeltron in the experimental apparatus is not independent of energy.

The major discrepancy between all the calculated and experimental polar angle distributions is for the intensity of the scattered flux perpendicular to the surface. The experimental results consistently exhibit a larger intensity than the predicted values. The scattering at this polar angle is strongly dependent on the arrangement of the atoms in the first and second layers. Any reconstruction of the W{100} surface would undoubtedly alter the scattered intensity perpendicular to the surface. Studies are underway to determine how sensitive these measurements may be to evaluating the microscopic nature of the W{100} reconstruction.

Acknowledgments

The financial support of the National Science Foundation and the Office of Naval Research is gratefully acknowledged. One of us (B.J.G.) also thanks the Alfred P. Sloan Foundation for a Research Fellowship and the Camille and Henry Dreyfus Foundation.

References

[1] See for example, W. Heiland, Appl. Surface Sci. 13 (1982) 282;
R.P.N. Bronckers and A.G.J. de Wit, Surface Sci. 104 (1981) 384; 112 (1982) 111, 133;
M. Aono, Y. Hou, C. Oshima and Y. Ishizawa, Phys. Rev. Letters 49 (1982) 567; 51 (1983) 801.
[2] T.M. Buck, G.H. Wheatley and L.K. Verheij, Surface Sci. 90 (1979) 635.
[3] T. v.d. Hagen and E. Bauer, Phys. Rev. Letters 47 (1981) 579.
[4] E. Taglauer, W. Englert, W. Heiland and D.P. Jackson, Phys. Rev. Letters 45 (1980) 740.
[5] B.M. DeKoven, S.H. Overbury and P.C. Stair, Phys. Rev. Letters 53 (1984) 481.
[6] H.B. Nielsen and T.A. Delchar, Surface Sci. 141 (1984) 487.
[7] B.J. Garrison, Surface Sci. 87 (1979) 683.
[8] B.J. Garrison and N. Winograd, Science 216 (1982) 805.
[9] K.E. Foley and B.J. Garrison, J. Chem. Phys. 72 (1980) 1018.
[10] C.-C. Chang, L.A. DeLouise, N. Winograd and B.J. Garrison, Surface Sci. 154 (1985) 22.
[11] C.-C. Chang, B.J. Garrison and N. Winograd, unpublished results.
[12] I.M. Torrens, Interatomic Potentials (Academic Press, New York, 1972).
[13] Recent papers on this topic include:
(a) J.A. Walker, M.K. Debe and D.A. King, Surface Sci. 104 (1981) 405;
(b) R.T. Tung, W.R. Graham and A.J. Melmed, Surface Sci. 115 (1982) 576;

(c) P.C. Stephenson and D.W. Bullett, Surface Sci. 139 (1984) 1;
and references therein.
[14] See, for example, W. Heiland, E. Taglauer and M.T. Robinson, Nucl. Instr. Methods 132 (1976) 655.
[15] S.H. Overbury, P.C. Stair and P.A. Agron, Surface Sci. 125 (1983) 377.
[16] H.F. Helbig, M.W. Linder, G.A. Morris and S.A. Steward, Surface Sci. 114 (1982) 251.
[17] I. Amdur, J.E. Jordan and S.O. Colgate, J. Chem. Phys. 34 (1961) 1525;
I. Amdur and J.E. Jordan, Advan. Chem. Phys. 10 (1966) 29.